1

2

LY6E Restricts the Entry of Human Coronaviruses, including the currently pandemic

SARS-CoV-2

5

Xuesen Zhao[1, 2, 4#]*, Shuangli Zheng[1, 2#], Danying Chen[1, 2], Mei Zheng[1, 2], Xinglin Li[1, 2] Guoli

Li[1,2], Hanxin Lin[3], Jinhong Chang[4], Hui Zeng[1, 2] and Ju-Tao Guo[4]*

8

[1]Institute of Infectious disease, Beijing Ditan Hospital, Capital Medical University, Beijing

100015, China. [2]Beijing Key Laboratory of Emerging Infectious Disease, Beijing 100015, China.

[3]Department of Pathology and Laboratory Medicine, Western University, 1151 Richmond Street,

London, Ontario, Canada. [4]Baruch S. Blumberg Institute, Hepatitis B Foundation, 3805 Old

Easton Road, Doylestown, PA 18902. USA.

.

Running Title: LY6E restricts human coronavirus entry

16

* Corresponding author's mailing address:

Xuesen Zhao, Beijing Ditan Hospital, Capital Medical University, Beijing, China. E-mail:

zhaoxuesen@ccmu.edu.cn

Ju-Tao Guo, Baruch S. Blumberg Institute, Doylestown, PA 18902. USA. E-mail: ju-

tao.guo@bblumberg.org

22

[#] These authors are co-first authors.

24

ABSTRACT

26   C3A is a sub-clone of human hepatoblastoma HepG2 cell line with the strong contact inhibition

27   of growth. We fortuitously found that C3A was more susceptible to human coronavirus HCoV-

28   OC43 infection than HepG2, which was attributed to the increased efficiency of virus entry into

29   C3A cells. In an effort to search for the host cellular protein(s) mediating the differential

30   susceptibility of the two cell lines to HCoV-OC43 infection, we found that ADAP2, GILT and

31   LY6E, three cellular proteins with known activity of interfering virus entry, expressed at

32   significantly higher levels in HepG2 cells. Functional analyses revealed that ectopic expression

33   of LY6E, but not GILT or ADAP2, in HEK 293 cells inhibited the entry of HCoV-OC43. While

34   overexpression of LY6E in C3A and A549 cells efficiently inhibited the infection of HCoV-

35   OC43, knockdown of LY6E expression in HepG2 significantly increased its susceptibility to

36   HCoV-OC43 infection. Moreover, we found that LY6E also efficiently restricted the entry

37   mediated by the envelope spike proteins of other human coronaviruses, including the currently

38   pandemic SARS-CoV-2. Interestingly, overexpression of serine protease TMPRSS2 or

39   amphotericin treatment significantly neutralized the IFITM3 restriction of human coronavirus

40   entry, but did not compromise the effect of LY6E on the entry of human coronaviruses. The

41   work reported herein thus demonstrates that LY6E is a critical antiviral immune effector that

42   controls CoV infection and pathogenesis *via* a distinct mechanism.

43 **Importance**

44

45 Virus entry into host cells is one of the key determinants of host range and cell tropism and is

46 subjected to the control by host innate and adaptive immune responses. In the last decade,

47 several interferon inducible cellular proteins, including IFITMs, GILT, ADAP2, 25CH and

48 LY6E, had been identified to modulate the infectious entry of a variety of viruses. Particularly,

49 LY6E was recently identified as host factors to facilitate the entry of several human pathogenic

50 viruses, including human immunodeficiency virus, influenza A virus and yellow fever virus.

51 Identification of LY6E as a potent restriction factor of coronaviruses expands the biological

52 function of LY6E and sheds new light on the immunopathogenesis of human coronavirus

53 infection.

54

INTRODUCTION

Coronaviruses (CoV) are a large family of enveloped positive-strand RNA viruses with broad host ranges and tissue tropism (1, 2). While four human CoVs, including HCoV-229E, HCoV-OC43, HCoV-NL63 and HCoV-HKU1, cause mild upper respiratory tract infections, three zoonotic CoVs have crossed species barriers to infect humans since 2002 and cause severe acute respiratory syndrome (SARS) (3, 4), Middle East respiratory syndrome (MERS) (5, 6) and coronaviral disease-19 (COVID-19) (7, 8), with the mortality rate of 10%, 30% and 1 to 2%, respectively (9, 10). No vaccine or antiviral drug is currently available to prevent CoV infection or treat the infected individuals. The cross-species transmission of zoonotic CoVs presents a continuous threat to global human health (11, 12). Therefore, understanding the mechanism of CoV infection and pathogenesis is important for the development of vaccines and antiviral agents to control the current COVID-19 pandemics and prevent future zoonotic CoV threats.

CoV entry into host cells, a process to deliver viral nucleocapsids cross the plasma membrane barrier into the cytoplasm, is the key determinant of virus host range and plays a critical role in zoonotic CoV cross-species transmission (2, 13). The entry process begins by the binding of viruses to their specific receptor on the plasma membrane, which triggers endocytosis to internalize the viruses into the endocytic vesicles. The cleavage of viral envelope spike proteins by endocytic proteases and/or endosomal acidification triggers the conformation change of spike protein to induce the fusion of viral envelope with endocytic membrane and release nucleocapsids into the cytoplasm to initiate viral protein synthesis and RNA replication. While angiotensin-converting enzyme 2 (ACE2) is the *bona fide* receptor for SARS-CoV, SARS-CoV-2 and HCoV-NL63 (14-16), MERS-CoV and HCoV-229E use dipeptidyl peptidase-4 (DPP4)

4

78   and CD13 (also known as aminopeptidase N) as their receptor, respectively (17, 18). However,

79   HCoV-OC43 and HCoV-HKU1 bind to 9-Oacetylated sialic acids *via* a conserved receptor-

80   binding site in spike protein domain A to initiate the infection of target cells (19). As the key

81   determinant of cell tropism, host range, and pathogenesis, CoV entry is primarily controlled by

82   interactions between the spike envelope glycoprotein and host cell receptor as well as the

83   susceptibility of spike glycoprotein to protease cleavage and/or acid-induced activation of

84   membrane fusion (20, 21). For instance, SARS-CoV can use ACE2 orthologs of different animal

85   species as receptors (22-26) and the efficiency of these ACE2 orthologs to mediate SARS-CoV

86   cell entry is consistent with the susceptibility of these animals to SARS-CoV infection (27-30).

87   In addition, expression of endosomal cathepsins, cell surface transmembrane proteases

88   (TMPRSS), furin, and trypsin differentially modulates the entry of different human CoVs (31-

89   35).

90   Interferons (IFNs) are the primary antiviral cytokines that mediate innate and adaptive

91   immune control of virus infection by inducing hundreds of genes, many of which encode

92   antiviral effectors (36). In the last decades, several IFN-inducible proteins, including three IFN-

93   induced   transmembrane   (IFITM)   proteins   (37),   gamma-interferon-inducible

94   lysosome/endosome-localized thiolreductase (GILT) (38), 25-Hydroxycholesterol hydrolase

95   (25HC) (39), ArfGAP with dual pleckstrin homology (PH) domains 2 (ADAP2) (40) and

96   lymphocyte antigen 6 family member E (LY6E) (41) had been identified to restrict or enhance

97   the entry of a variety of viruses. Interestingly, while IFITM proteins inhibit the entry of all the

98   other human CoVs, HCoV-OC43 hijacks human IFITM2 or IFITM3 as entry factors to facilitate

99   its infection of host cells (42, 43). We also demonstrated recently that GILT suppresses the entry

100   of SARS-CoV, but not other human CoVs (38). As reported herein, in our efforts to identify host

101   factor(s) determining the differential susceptibility of two closed related human hepatoma cell

102   lines to HCoV-OC43 infection, we found that LY6E potently suppresses the infectious entry of

103   all the human CoVs, including the currently pandemic SARS-COV-2. Our study also revealed

104   that unlikely IFITMs, LY6E inhibits CoV entry *via* a distinct mechanism.

105

106   **RESULTS**

107

108   **C3A is more susceptible to HCoV-OC43 infection than its parental cell line HepG2.** C3A is

109   a sub-clone of HepG2 that was selected for strong contact inhibition of growth and high albumin

110   production (44). Metabolically, C3A is more relevant to normal hepatocytes and has been used

111   for development of bioartificial liver devices (45). Interestingly, we found that these two closely

112   related cell lines drastically differ in their susceptibility to HCoV-OC43 infection (Fig. 1).

113   Specifically, infection of the two cell lines with the virus at a MOI of 0.02, 0.2 and 1 resulted in

114   approximately 75, 25 and 10 folds more infected cells in C3A cultures than in HepG2 cultures at

115   24 h post infection, respectively (Fig. 1A). Consistent with this finding, much higher levels of

116   viral nucleocapsid protein (N) and RNA were detected in infected C3A cultures (Figs. 1B and C).

117   Infected C3A cultures also produced approximately 20-fold more progeny viruses than HepG2

118   cultures did (Fig. 1D). To determine whether the differential susceptibility of the two hepatoma

119   cell lines to HCoV-OC43 infection is due to a difference in virus entry or post-entry replication

120   event, we compared the susceptibility of the two cell lines to lentiviral particles pseudotyped

121   with envelope proteins of HCoV-OC43, influenza A virus (IAV), vesicular stomatitis virus (VSV)

122   or Lassa fever virus (LASV). As shown in Fig 2, while pseudoviral particles of IAV (IAVpp),

123   VSV (VSVpp) and LASV (LASVpp) infected the two cell lines with similar efficiency, the

6

124   efficiency of HCoV-OC43pp infection in C3A cultures is approximately 50 folds higher than

125   that in HepG2 cultures. These results clearly indicate that the differential susceptibility is

126   attributed to the distinct ability of the two cell lines to support the infectious entry of HCoV-

127   OC43.

128

129   **IFITM proteins modulate HCoV-OC43 infection of C3A and HepG2 cells in a similar**

130   **extent.** We reported previously that IFITM proteins differentially modulate HCoV-OC43 entry

131   into target cells. While IFITM1 inhibits the virus entry, IFITM2 and IFITM3 enhance the cellular

132   entry of this virus (42). To investigate whether the differential expression of IFITM proteins in

133   the two cell lines is responsible for their difference in HCoV-OC43 infection efficiency, we

134   examined IFITM protein expression by Western blot assays and found the two hepatoma cell

135   lines expressed similar levels of IFITM1 and IFITM2/3 (Fig. 1B). Because the C-terminal

136   variable regions of IFITM1 and IFITM3 control the inhibition and enhancement of HCoV-OC43

137   entry (42), respectively, we further compared the effects of IFITM1 and C-terminal region

138   exchanged IFITM proteins on the virus infection. As shown in Fig. 3, in spite of their distinct

139   susceptibility, expression of IFITM1-EX2, a mutant IFITM1 protein with its C-terminal domain

140   replaced with the C-terminal domain of IFITM3 (42), and IFITM3-EX2, a mutant IFITM3

141   protein with its C-terminal domain replaced with the C-terminal domain of IFITM1 (42),

142   significantly enhanced and inhibited HCoV-OC43 infection of both cell lines, respectively, as

143   evidenced by the significant changes in infected cell percentage (Fig. 3A), reduced viral

144   nucleocapsid protein expression (Fig. 3B), intracellular RNA accumulation (Fig. 3C) and yields

145   of progeny virus production (Fig. 3D). Moreover, pseudotyped lentiviral infection assay further

146   demonstrated that IFITM1, IFITM1-EX2 and IFITM3-EX2 modulated HCoV-OC43 envelope

7

147   proteins mediated entry in a similar extent in the two cell lines (Fig. 3E). Accordingly, we

148   concluded that IFITM proteins were not responsible for the observed differential susceptibility of

149   the two hepatoma cell lines to HCoV-OC43 infection.

150

151   **LY6E inhibits the entry mediated by human CoV envelope spike proteins and is**

152   **responsible for the differential susceptibility of C3A and HepG2 cells to HCoV-OC43**

153   **infection.** In order to identify host cellular proteins that may enhance HCoV-OC43 infection of

154   C3A cells or suppress the virus entry into HepG2 cells, we first compared the expression of

155   several cellular genes with known activity to restrict or enhance virus entry into target cells. As

156   shown in Fig. 4A, we found that ADAP2, GILT and LY6E mRNA expressed at significantly

157   higher levels in HepG2 cells. While the expression of ADAP2 and GILT did not inhibit HCoV-

158   OC43pp infection (Fig. 4B), expression of LY6E in Flp-In TREx 293 cells efficiently suppressed

159   the infection of lentiviral particles pseudotyped with the envelope glycoproteins of all the human

160   CoVs including SARS-CoV-2, except for SARS-CoV (Fig. 4C and 4D). In addition, LY6E

161   enhanced the infection of IAVpp (Fig. 4D). In agreement with our previous report, expression of

162   GILT inhibited SARS-CoVpp infection (38). To further confirm the role of LY6E in HCoV-

163   OC43 infection, we showed that ectopic expression of LY6E in C3A and A549 cells

164   significantly reduced their susceptibility to the virus infection, whereas reducing the expression

165   of LY6E in HepG2 cells by shRNA knockdown significantly increased HCoV-OC43 infection

166   (Fig. 5). The results presented above imply that LY6E is a restriction factor for human CoVs and

167   responsible for the differential susceptibility of C3A and HepG2 cells to HCoV-OC43 infection.

168

8

169 **LY6E restriction of human coronavirus entry depends on GPI-anchor and the**

170 **evolutionally conserved L36 residue.** LY6E is a member of the LY6/uPAR superfamily. Like

171 most LY6 family members, LY6E contains ten cysteines that form a highly conserved, three-

172 finger folding motif through disulfide bonding and localizes on the plasma membrane of cells *via*

173 glycosylphosphatidylinositol (GPI) anchoring. LY6E is ubiquitously expressed in many cell

174 types and functions in modulation of cell signal transduction (41). Recent studies revealed that

175 human LY6E promotes the entry of HIV (46, 47) and multiple enveloped RNA viruses from

176 several viral families (48). Moreover, the enhancement of RNA viral infection is a conserved

177 function of all the mammalian LY6E orthologs examined thus far. Particularly, substitution of

178 the evolutionally conserved residue L36 with alanine (A) completely abolished the viral

179 enhancement activity of LY6E (48). Interestingly, we found that L36A substitution also

180 abolished the activity of LY6E to restrict the entry of human CoVs (Fig. 6). As anticipated,

181 N99A substitution that disrupts the addition of GPI anchor also abrogated the inhibitory effects

182 of LY6E on human CoV entry (Fig. 6). These results indicate that proper interaction of LY6E

183 with other viral/cellular components *via* the conserved residue L36 and localization in the

184 specific cell membrane microdomians are required for LY6E restriction of human CoV entry.

185

186 **Activation of CoV entry by TMPRSS2 expression fails to evade LY6E restriction of CoV**

187 **entry.** It was reported by others and us that expression of cell membrane associated serine

188 protease TMPRSS2 enhances SARS-CoV and SARS-like bat CoV entry (32-34). More

189 importantly, the TMPRSS2-enhanced entry can evade IFITM3 restriction (*Mei Zheng, et al,*

190 *manuscript under review*), presumably because the cellular protease activates the viral fusion at

191 cell surface or early endosomes where IFITM3 expression at a relatively lower levels and thus

192   fails to inhibit viral fusion. To determine the effects of TMPRSS2 expression on LY6E

193   restriction of human CoV entry, Flp-In TREx 293-derived cell line expressing LY6E were

194   transfected with a control vector (pCAGGS) or a plasmid expressing human TMPRSS2 and

195   cultured in the absence or presence of tetracycline (tet) for 24 h. The cells were then infected

196   with the indicated pseudotyped lentiviruses. As shown in Fig. 7A, in absence of tet to induce

197   LY6E, expression of TMPRSS2 significantly enhanced the infection of SARS-CoVpp, MERS-

198   CoVpp and HCoV-229Epp, but not the infection of other human CoVpp and LASVpp.

199   Interestingly, LY6E significantly inhibited the infection of MERS-CoVpp and HCoV-229Epp in

200   the cells without or with ectopic expression of TMPRSS2. Moreover, LY6E failed to inhibit

201   SARS-CoVpp infection in the absence of TMPRSS2 expression, but significantly inhibited

202   SARS-CoVpp infection in the cells expressing TMPRSS2 (Fig. 7B). Therefore, unlikely IFITM3,

203   expression of TMPRSS2 cannot evade LY6E restriction of human CoV entry. Instead, LY6E

204   restriction of the entry of human CoVs, particularly SARS-CoV, is regulated by the expression

205   of cellular proteases that previously known to activate the fusion activity of viral spike proteins.

206

207   **Amphotericin B treatment does not compromise LY6E restriction of human CoV entry.**

208   Amphotericin B (AmphoB) is antifungal medicine that binds with ergosterol in fungal cell

209   membranes, forming pores that cause rapid leakage of monovalent ions and subsequent fungal

210   cell death. AmphoB can also bind to cholesterol in mammalian cell membrane, albeit at a lesser

211   affinity than to fungal ergosterol (49). The cholesterol-enriched plasma membrane microdomains

212   known as lipid rafts play important roles in the entry and egress of many enveloped viruses (50,

213   51). Particularly, AmphoB treatment had been shown to significantly compromise IFITM

214   restriction of IAV entry (52) and attenuate IFITM enhancement of HCoV-OC43 infection (42).

215   In this study, we further demonstrated that AmphoB treatment also efficiently attenuated the

216   restriction of IFITM3 on the infection of SARS-CoVpp, MERS-CoVpp, HCoV-NL63pp, HCoV-

217   229Epp and IAVpp, but not LASVpp (Fig. 8A). However, AmphoB treatment altered neither the

218   restriction activity of LY6E on the infection of human CoV spike protein-pseudotyped

219   lentiviruses nor the enhancement of LY6E on IAVpp infection (Fig. 8B). These results strongly

220   imply that LY6E modulates virus entry *via* a distinct mechanism.

221

222   **DISCUSSION**

223

224   LY6E was initially identified as a cell surface marker to discriminate immature from

225   mature thymocytes subsets (53). The primary function of LY6E has been associated with

226   immune regulation, specifically in modulating T cell activation, proliferation, development (54).

227   In addition to lymphocytes, LY6E mRNA can also be detected in liver, spleen, uterus, ovary,

228   lung, and brain and its expression can be induced by type I IFN in a cell-type specific manner

229   (53). However, LY6E is not a typical antiviral effector protein. Instead, LY6E was reported to

230   promote the infection of enveloped RNA viruses from several viral families (48) and modulates

231   HIV-1 infection in a manner dependent on the level of CD4 expression in target cells (46, 47).

232   Our finding that LY6E restricts human CoV infection and characterization of its antiviral effects

233   shed new lights on the mode of LY6E action on virus entry in general.

234   First, either the enhancement or restriction of LY6E on virus entry depends on its GPI

235   anchor (Fig. 6) (46-48). GPI-anchored proteins are preferentially located in lipid rafts, the plasma

236   membrane microdomains enriched in glycosphingolipids and cholesterol as well as protein

237   receptors or ligands. Lipid rafts are considered to compartmentalize membrane processes by

11

238   facilitating the interaction of protein receptors and their ligands/effectors to modulate membrane

239   functions, such as signal transduction, membrane fusion, vesicle budding and trafficking. Lipid

240   rafts also involve in the entry and egress of many viruses. For instance, both HIV-1 receptor

241   (CD4) and coreceptors are localized in lipid rafts. Yu and colleagues elegantly demonstrated

242   recently that LY6E enhances HIV-1 infection of CD4+ T cells and monocytic THP1- cells by

243   promoting the expansion of viral fusion pore induced by HIV-1 Env (47). Furthermore, LY6E

244   was found to be the receptor of mouse endogenous retroviral envelope Syncytin-A and

245   interaction of LY6E with Syncytin-A induces the syncytiotrophoblast fusion and placental

246   morphogenesis (55, 56). However, Mar and colleagues showed that LY6E enhances IAV

247   infection of cells by promoting a viral replication step after viral nucleocapsid escape from

248   endosomes, but before viral RNP nuclear translocation, *i.e.*, most likely the uncoating of

249   nucleocapsids (48). Interestingly, the results presented in Fig. 4 indicate that LY6E significantly

250   enhanced the infection of IAVpp, suggesting that the LY6E enhancement of IAV infection is, at

251   least in part, through promoting the entry into target cells, possibly also by enhancing viral

252   fusion. Considering the broad inhibitory effects of LY6E on human CoVs and its fusogenic or

253   fusion-modulating activity, we speculate that LY6E might inhibit the membrane fusion triggered

254   by CoV spike proteins. However, the role of LY6E on endocytosis and endocytic vesicle

255   trafficking cannot be ruled out. These hypotheses are currently under investigation.

256   Second, in addition to GPI anchor, the evolutionally conserved amino acid residue L36 is

257   also required for both the enhancement and restriction of virus entry into target cells by LY6E

258   (Fig. 6) (48). It can be speculated that this specific residue may mediate an interaction with other

259   cellular membrane proteins to module viral entry. The fact that LY6E enhances viral infectivity

260   in a cell type-specific manner, with the strongest phenotype in cells of fibroblast and monocytic

261   lineages (48), does indicate the involvement of other host cellular factors. Variations in the

262   abundance of expression, as well as the localization of LY6E and its associated proteins or lipids,

263   may explain the differential effects of LY6E on the infection of different viruses in different cell

264   types (Fig. 4 and 7). However, LY6E enhancement of RNA virus infection appears to be

265   independent of type I interferon response and other ISG expression (48). Particularly,

266   enhancement of viral infection in Huh7.5 cells that do not have basal levels of IFITM protein

267   expression indicates that LY6E enhancement of RNA viral infection is most likely not through

268   modulating the function of IFITM proteins (42). This notion is further supported by the finding

269   that LY6E and Syncitin-A mediated syncytiotrophoblast fusion can be inhibited by IFITM

270   proteins (57, 58).

271   Third, studying the effects of LY6E on HIV-1 infection of CD4 low-expressing cells,

272   such as Jurkat T cells and primary monocyte-derived macrophages, revealed that HIV-1 entry

273   was inhibited by LY6E (46). This appears due to the LY6E-induced reduction of lipid raft-

274   associated CD4 on the surface of these cells. It was demonstrated that LY6E can promote CD4

275   endocytosis and mobilize lipid raft-associated CD4 molecules to non-raft microdomains. Such a

276   receptor down-regulation significantly reduced HIV-1 binding and infection of CD4 low-

277   expressing cells (macrophages), but did not significantly impact the binding of HIV-1 to CD4

278   high-expressing cells, which allows for LY6E to predominantly enhance HIV-1 infection of

279   CD4+ T lymphocytes by promotion of membrane fusion (46). It is, therefore, possible that LY6E

280   inhibition of human CoV infection is due to the down-regulation of lipid raft-associated CoV

281   receptors. However, the differential effects of LY6E on the infection of SARS-CoVpp, SARS-

282   CoV-2pp and HCoV-NL63pp, that share the ACE2 receptor, does not support such a hypothesis

283   (Fig. 4).

284   Finally, the findings that LY6E inhibits human CoV entry cannot be evaded by ectopic

285   expression of membrane-associated serine protease TMPRSS2 and compromised by AmphoB

286   treatment strongly indicate that LY6E modulates virus entry *via* a distinct mechanism from that

287   IFITM proteins do (Figs. 7 and 8). Specifically, inhibition of TMPESS2-enhanced CoV entry

288   implies that LY6E most likely blocks virus entry at plasma membrane or in early endosomes.

289   Moreover, IFITMs impede viral fusion by decreasing membrane fluidity and curvature (37).

290   AmphoB can bind cholesterol in cell membranes to increase membrane fluidity and planarity and

291   consequentially rescue IFITM inhibition of virus entry (52). Interestingly, AmphoB only

292   neutralize the antiviral effects of IFITM2 and IFITM3, but has little effect on IFITM1 restriction

293   of virus entry (52). While IFITM1 is predominantly located in the plasma membrane or early

294   endosomes, IFITM2 and 3 are mainly localized in the later endosomes and lysosomes. Due to

295   their differential subcellular localization, IFITM1 mainly restricts the viruses that enter the cells

296   at cell surface or in the early endosomes, such as parainfluenza viruses and hepatitis C virus (59,

297   60), IFITM2 and 3 primarily restrict the infection of viruses that enter the cells at later

298   endosomes and/or lysosomes (43, 61, 62). Because AmphoB is endocytosed quite rapidly

299   leading to its concentration in the late endosomes and lysosomes, it more efficiently alleviates

300   the effect of IFITM2 and 3, but not IFITM1, on virus entry (52). Similarly, the failure of

301   AmphoB to attenuate the antiviral effects of LY6E against human CoVs is most likely due to its

302   predominant cell surface localization and inhibition of an early step of CoV entry.

303   In summary, while it is very interesting to know that LY6E is capable of modulating the

304   entry of many RNA viruses, we only begin to uncover the mechanism of this fascinating host

305   factor and define its pathobiological role in virus infection (41, 63). Further understanding the

306 role and mechanism of LY6E in viral infections will establish a scientific basis for development

307 of therapeutics to harness its function for the treatment of viral diseases.

308

309 **MATERIALS AND METHODS**

310

311 **Cell culture.** Human hepatoma cell lines HepG2 and C3A, a sub-clone of HepG2 (ATCC HB-

312 8065) were purchased from ATCC and cultured in DMEM/F12 medium supplemented with 10%

313 heat-inactivated fetal bovine serum (FBS) (Invitrogen). Lung cancer cell line A549 were

314 obtained from ATCC and maintained in DMEM supplemented with 10% FBS. GP2-293 and

315 Lenti-X 293T cell Lines were purchased from Clontech and cultured in DMEM supplemented

316 with 10% FBS and 1 mM Sodium pyruvate (Invitrogen). Flp-In TREx 293 cells were purchased

317 from Invitrogen and maintained in DMEM supplemented with 10% FBS, 10 μg/ml blasticidin

318 (Invitrogen) and 100 µg/ml Zeocin (Invivogen) (64). Flp-In TREx 293-derived cell lines

319 expressing LY6E, GILT, ADAP2, or IFITM3 were cultured in DMEM supplemented with 10%

320 FBS, 5 μg/ml blasticidin and 250 μg/ml hygromycin.

321

322 **Viruses**. HCoV-OC43 (strain VR1558) were purchased from ATCC and amplified in HCT-8

323 cells according to the instruction from ATCC. Virus titers were determined by a plaque assay as

324 described previously (42).

325

326 **Antibodies.** Monoclonal antibody against FLAG tag (ANTI-FLAG M2) and β-Actin were

327 purchased from Sigma (Cat.No. F1804 and A2228, respectively). Monoclonal antibody against

328 human IFITM1 (Cat.No. 60047-1), rabbit polyclonal antibody against human IFITM3 (Cat.No.

15

329   11714-1-AP), which also efficiently recognizes IFITM2 and weakly cross-reacts with IFITM1,

330   were purchased from Proteintech Group, Inc. Mouse monoclonal antibody against HCoV-OC43

331   nucleocapsid (NP) protein was purchased from Millipore (Cat.No. MAB9012). Rabbit

332   polyclonal antibody against human LY6E was obtained from proteintech (Cat.No. 22144-1-AP).

333

334   **Plasmid construction.** The cDNA molecules of ADAP2 and LY6E were purchased from

335   OriGene (Cat. No. RC207501 and RC211373, respectively**)** and cloned into pcDNA5/FRT-

336   derived vector as described previously (42). Ly6E and N-terminally FLAG-tagged human

337   IFITM1, IFITM3 and their mutants were cloned into pQCXIP vector (Clontech) between the

338   NotI and BamHI sites as previously described (42, 43). pcDNA5/FRT-derived plasmids

339   expressing chloramphenicol acetyltransferase (CAT), N-terminally FLAG-tagged human

340   IFITM3 were reported previously (64-66).

341   Plasmids expressing HCoV-OC43 spike (S) and HE proteins, VSV G protein, H1N1 IAV

342   (A/WSN/33) hemagglutinin (HA) and neuraminidase (NA), LASV GP protein, murine leukemia

343   virus (MLV) envelope protein, HCoV-NL63, HCoV-229E, SARS-CoV and MERS-CoV spike

344   protein were described previously (67, 68). The codon-optimized (for human cells) SARS-CoV-

345   2 spike gene, which is based on NCBI Reference Sequence YP_009724390.1, was purchased

346   from GeneScript and cloned into pCAGGS vector as described previously (69). pRS-derived

347   retroviral vectors expressing a scramble shRNA and shRNA targeting the mRNA of human

348   LY6E were obtained from OriGene (Cat. No. TR311641).

349   Plasmid pNL4-3.Luc.R$^-$E$^-$ was obtained through the NIH AIDS Research and Reference

350   Reagent Program (70, 71). Angiotensin I converting enzyme 2 (ACE2), aminopeptidase N

351   (APN), and dipeptidyl peptidase-4 (DPP4) cDNA clones were obtained from Origene, and

16

352   cloned into a pcDNA3 vector (Invitrogen) to yield plasmid pcDNA3 /ACE2, pcDNA3 /APN and

353   pcDNA3/DDP4, respectively (69).

354

355   **Package of pseudotyped retroviral particles.** The various viral envelope protein pseudotyped

356   lentiviruses bearing luciferase reporter gene as well as VSV G protein pseudotyped Moloney

357   murine leukemia virus (MMLV)-derived retroviral vectors (pQCXIP) expressing wild-type and

358   mutant human IFITM, LY6E, or pRS vector-derived plasmid expressing a scrambled shRNA or

359   shRNA specifically targeting human LY6E were packaged as reported previously . Each

360   pseudotype was titrated by infection of cells with a serial dilution of pseudotype preparations.

361   The modulation of IFITM or LY6E on the transduction of a given pseudotype was determined

362   with a titrated amount of pseudotypes that yield luciferase signal between 10,000 to 1,000,000

363   light units per well of 96-well plates (69, 72). For a given pseudotype, the input of pseudoviral

364   particles is consistent across all the experiments.

365

366   **Establishment of cell lines stably expressing wild-type and mutant IFITM or LY6E**

367   **proteins or shRNA.** HepG2, C3A or A549 cells in each well of 6-well plates were incubated

368   with 2 ml of Opti-MEM medium containing pseudotyped retroviruses and centrifuged at 20 °C

369   for 30 minutes at 4,000×g. Forty-eight hours post transduction, cells were cultured with media

370   containing 2 µg/ml of puromycin for two weeks. The antibiotic resistant cells were pooled and

371   expanded into cell lines stably expressing wild-type or mutant IFITM or LY6E proteins or

372   shRNA targeting LY6E. Flp-In TREx 293-derived cell lines expressing IFITM, GILT, ADAP2

373   or LY6E proteins in a tetracycline (tet) inducible manner were established as previously

374   described (64, 66).

17

375

376   **Immunofluorescence.** To visualize HCoV-OC43 infected cells, the infected cultures were fixed

377   with 2% paraformaldehyde for 10 min. After permeabilization with 0.1% Triton X-100, the cells

378   were stained with a monoclonal antibody (541-8F) recognizing HCoV-OC43 NP protein. The

379   bound antibodies were visualized by using Alexa Fluor 488-labeled (green) goat anti-mouse IgG

380   or Alexa Fluor 555-labeled (red) goat anti-mouse IgG, Cell nuclei were counterstained with

381   DAPI.

382

383   **Western blot assay.** Cells were lysed with $1\times$ Laemmli buffer. An aliquot of cell lysate was

384   separated on NuPAGE® Novex 4-12% Bis-Tris Gel (Invitrogen) and electrophoretically

385   transferred onto a nitrocellulose membrane (Invitrogen). The membranes were blocked with PBS

386   containing 5% nonfat dry milk and probed with the desired antibody. The bound antibodies were

387   visualized with IRDye secondary antibodies and imaging with LI-COR Odyssey system (LI-

388   COR Biotechnology).

389

390   **Real-time RT-PCR.** HCoV-OC43 RNA was quantified by a qRT-PCR assay described

391   previously (42). To determine the level of ISG mRNA, total cellular RNA was extracted using

392   TRIzol reagent (Invitrogen) and the same amount of total cellular RNA was reverse-transcribed

393   with SuperScript III kit ((Invitrogen). Quantitative RT-PCR was performed using iTaq universal

394   SYBR Green Supermix (Bio-Rad) with the following primers: LY6E, 5´-

395   GTACTGCCTGAAGCCGACCATC-3´ and 5´-AGATTCCCAATGCCGGCACTAG-3´;

396   ADAP2, 5´-AGCTGTCATCAGCATTAAG-3´ and 5´-ACTATCTCCTTCCCACTTTC-3´;

397   GILT, 5´-AATGTGACCCTCTACTATGAAG-3´ and 5´-

18

398   ACGCTGGTGCCCTACGGAAACG-3´; GAPDH, 5´-GAAGGTGAAGGTCGGAGTCAAC-3

399   ´ and 5´-CAGAGTTAAAAGCAGCCCTGGT-3´. Gene expression was calculated using the $2^{-\triangle}$

400     $^{\triangle CT}$ method, normalized to GAPDH as described previously (31, 40).

401

402   **Luciferase assay.** Flp-In TREx 293-derived IFITM-expressing cell lines were seeded into 96-

403   well plates with black wall and clear bottom and transfected with an empty vector plasmid or

404   plasmids encoding ACE2, APN, or DPP4 to express viral receptors. For Huh7.5-derived IFITM-

405   expressing cell lines, cells were seeded into black wall 96-well plates. Cells were infected at 24 h

406   post transfection or infected with desired pseudotyped lentiviral particles for 2 h, and then

407   replenished with fresh media. Two days post infection, the media were removed and cells were

408   lysed with 20 µl/well of cell lysis buffer (Promega) for 15 min, followed by adding 50 µl/well of

409   luciferase substrate (Promega). The firefly luciferase activities were measured by luminometry in

410   a TopCounter (Perkin Elmer) (69).

411

412   **Statistical analyses** All the experiments were repeated at least three times. Differences between

413   control sample and tests were statistically analyzed using Student's t tests or one-way analysis of

414   variance (ANOVA). p-values less than 0.05 were considered statistically significant.

415

416 **Funding Information**

421

REFERENCES

1. **Weiss SR, Navas-Martin S.** 2005. Coronavirus pathogenesis and the emerging pathogen severe acute respiratory syndrome coronavirus. Microbiol Mol Biol Rev **69:**635-664.

2. **Peck KM, Burch CL, Heise MT, Baric RS.** 2015. Coronavirus Host Range Expansion and Middle East Respiratory Syndrome Coronavirus Emergence: Biochemical Mechanisms and Evolutionary Perspectives. Annu Rev Virol **2:**95-117.

3. **Ksiazek TG, Erdman D, Goldsmith CS, Zaki SR, Peret T, Emery S, Tong S, Urbani C, Comer JA, Lim W, Rollin PE, Dowell SF, Ling AE, Humphrey CD, Shieh WJ, Guarner J, Paddock CD, Rota P, Fields B, DeRisi J, Yang JY, Cox N, Hughes JM, LeDuc JW, Bellini WJ, Anderson LJ, Group SW.** 2003. A novel coronavirus associated with severe acute respiratory syndrome. N Engl J Med **348:**1953-1966.

4. **Rota PA, Oberste MS, Monroe SS, Nix WA, Campagnoli R, Icenogle JP, Penaranda S, Bankamp B, Maher K, Chen MH, Tong S, Tamin A, Lowe L, Frace M, DeRisi JL, Chen Q, Wang D, Erdman DD, Peret TC, Burns C, Ksiazek TG, Rollin PE, Sanchez A, Liffick S, Holloway B, Limor J, McCaustland K, Olsen-Rasmussen M, Fouchier R, Gunther S, Osterhaus AD, Drosten C, Pallansch MA, Anderson LJ, Bellini WJ.** 2003. Characterization of a novel coronavirus associated with severe acute respiratory syndrome. Science **300:**1394-1399.

5. **Zaki AM, van Boheemen S, Bestebroer TM, Osterhaus AD, Fouchier RA.** 2012. Isolation of a novel coronavirus from a man with pneumonia in Saudi Arabia. N Engl J Med **367:**1814-1820.

6. **van Boheemen S, de Graaf M, Lauber C, Bestebroer TM, Raj VS, Zaki AM, Osterhaus AD, Haagmans BL, Gorbalenya AE, Snijder EJ, Fouchier RA.** 2012. Genomic characterization of a newly discovered coronavirus associated with acute respiratory distress syndrome in humans. mBio **3**.

7. **Wu F, Zhao S, Yu B, Chen YM, Wang W, Song ZG, Hu Y, Tao ZW, Tian JH, Pei YY, Yuan ML, Zhang YL, Dai FH, Liu Y, Wang QM, Zheng JJ, Xu L, Holmes EC, Zhang YZ.** 2020. A new coronavirus associated with human respiratory disease in China. Nature **579:**265-269.

8. **Zhou P, Yang XL, Wang XG, Hu B, Zhang L, Zhang W, Si HR, Zhu Y, Li B, Huang CL, Chen HD, Chen J, Luo Y, Guo H, Jiang RD, Liu MQ, Chen Y, Shen XR, Wang X, Zheng XS, Zhao K, Chen QJ, Deng F, Liu LL, Yan B, Zhan FX, Wang YY, Xiao GF, Shi ZL.** 2020. A pneumonia outbreak associated with a new coronavirus of probable bat origin. Nature **579:**270-273.

9. **Zhu N, Zhang D, Wang W, Li X, Yang B, Song J, Zhao X, Huang B, Shi W, Lu R, Niu P, Zhan F, Ma X, Wang D, Xu W, Wu G, Gao GF, Tan W, China Novel Coronavirus I, Research T.** 2020. A Novel Coronavirus from Patients with Pneumonia in China, 2019. N Engl J Med **382:**727-733.

10. **Lu R, Zhao X, Li J, Niu P, Yang B, Wu H, Wang W, Song H, Huang B, Zhu N, Bi Y, Ma X, Zhan F, Wang L, Hu T, Zhou H, Hu Z, Zhou W, Zhao L, Chen J, Meng Y, Wang J, Lin Y, Yuan J, Xie Z, Ma J, Liu WJ, Wang D, Xu W, Holmes EC, Gao GF, Wu G, Chen W, Shi W, Tan W.** 2020. Genomic characterisation and epidemiology of 2019 novel coronavirus: implications for virus origins and receptor binding. Lancet **395:**565-574.

467   11.   **Menachery VD, Yount BL, Jr., Debbink K, Agnihothram S, Gralinski LE, Plante**
468   **JA, Graham RL, Scobey T, Ge XY, Donaldson EF, Randell SH, Lanzavecchia A,**
469   **Marasco WA, Shi ZL, Baric RS.** 2015. A SARS-like cluster of circulating bat
470   coronaviruses shows potential for human emergence. Nat Med **21:**1508-1513.
471   12.   **Wan Y, Shang J, Graham R, Baric RS, Li F.** 2020. Receptor recognition by novel
472   coronavirus from Wuhan: An analysis based on decade-long structural studies of SARS. J
473   Virol doi:10.1128/JVI.00127-20.
474   13.   **Sheahan T, Rockx B, Donaldson E, Sims A, Pickles R, Corti D, Baric R.** 2008.
475   Mechanisms of zoonotic severe acute respiratory syndrome coronavirus host range
476   expansion in human airway epithelium. J Virol **82:**2274-2285.
477   14.   **Li W, Moore MJ, Vasilieva N, Sui J, Wong SK, Berne MA, Somasundaran M,**
478   **Sullivan JL, Luzuriaga K, Greenough TC, Choe H, Farzan M.** 2003. Angiotensin-
479   converting enzyme 2 is a functional receptor for the SARS coronavirus. Nature **426:**450-
480   454.
481   15.   **Hofmann H, Pyrc K, van der Hoek L, Geier M, Berkhout B, Pohlmann S.** 2005.
482   Human coronavirus NL63 employs the severe acute respiratory syndrome coronavirus
483   receptor for cellular entry. Proc Natl Acad Sci U S A **102:**7988-7993.
484   16.   **Hoffmann M, Kleine-Weber H, Schroeder S, Kruger N, Herrler T, Erichsen S,**
485   **Schiergens TS, Herrler G, Wu NH, Nitsche A, Muller MA, Drosten C, Pohlmann S.**
486   2020. SARS-CoV-2 Cell Entry Depends on ACE2 and TMPRSS2 and Is Blocked by a
487   Clinically Proven Protease Inhibitor. Cell doi:10.1016/j.cell.2020.02.052.
488   17.   **Raj VS, Mou H, Smits SL, Dekkers DH, Muller MA, Dijkman R, Muth D, Demmers**
489   **JA, Zaki A, Fouchier RA, Thiel V, Drosten C, Rottier PJ, Osterhaus AD, Bosch BJ,**
490   **Haagmans BL.** 2013. Dipeptidyl peptidase 4 is a functional receptor for the emerging
491   human coronavirus-EMC. Nature **495:**251-254.
492   18.   **Lachance C, Arbour N, Cashman NR, Talbot PJ.** 1998. Involvement of
493   aminopeptidase N (CD13) in infection of human neural cells by human coronavirus 229E.
494   J Virol **72:**6511-6519.
495   19.   **Hulswit RJG, Lang Y, Bakkers MJG, Li W, Li Z, Schouten A, Ophorst B, van**
496   **Kuppeveld FJM, Boons GJ, Bosch BJ, Huizinga EG, de Groot RJ.** 2019. Human
497   coronaviruses OC43 and HKU1 bind to 9-O-acetylated sialic acids via a conserved
498   receptor-binding site in spike protein domain A. Proc Natl Acad Sci U S A **116:**2681-
499   2690.
500   20.   **Gallagher TM, Buchmeier MJ.** 2001. Coronavirus spike proteins in viral entry and
501   pathogenesis. Virology **279:**371-374.
502   21.   **Millet JK, Whittaker GR.** 2015. Host cell proteases: Critical determinants of
503   coronavirus tropism and pathogenesis. Virus research **202:**120-134.
504   22.   **Chen Y, Liu L, Wei Q, Zhu H, Jiang H, Tu X, Qin C, Chen Z.** 2008. Rhesus
505   angiotensin converting enzyme 2 supports entry of severe acute respiratory syndrome
506   coronavirus in Chinese macaques. Virology **381:**89-97.
507   23.   **Guo H, Guo A, Wang C, Yan B, Lu H, Chen H.** 2008. Expression of feline angiotensin
508   converting enzyme 2 and its interaction with SARS-CoV S1 protein. Res Vet Sci **84:**494-
509   496.
510   24.   **Heller LK, Gillim-Ross L, Olivieri ER, Wentworth DE.** 2006. Mustela vison ACE2
511   functions as a receptor for SARS-coronavirus. Adv Exp Med Biol **581:**507-510.

512   25.   **Xu L, Zhang Y, Liu Y, Chen Z, Deng H, Ma Z, Wang H, Hu Z, Deng F.** 2009. The
513   Angiotensin Converting Enzyme 2 (ACE2) from Raccoon Dog can serve as an efficient
514   Receptor for the Spike Protein of Severe Acute Respiratory Syndrome Coronavirus. J
515   Gen Virol doi:vir.0.013490-0 [pii]
516   10.1099/vir.0.013490-0.
517   26.   **Zamoto A, Taguchi F, Fukushi S, Morikawa S, Yamada YK.** 2006. Identification of
518   ferret ACE2 and its receptor function for SARS-coronavirus. Adv Exp Med Biol
519   **581:**519-522.
520   27.   **Guan Y, Zheng BJ, He YQ, Liu XL, Zhuang ZX, Cheung CL, Luo SW, Li PH,**
521   **Zhang LJ, Guan YJ, Butt KM, Wong KL, Chan KW, Lim W, Shortridge KF, Yuen**
522   **KY, Peiris JS, Poon LL.** 2003. Isolation and characterization of viruses related to the
523   SARS coronavirus from animals in southern China. Science **302:**276-278.
524   28.   **Martina BE, Haagmans BL, Kuiken T, Fouchier RA, Rimmelzwaan GF, Van**
525   **Amerongen G, Peiris JS, Lim W, Osterhaus AD.** 2003. Virology: SARS virus
526   infection of cats and ferrets. Nature **425:**915.
527   29.   **Qin C, Wang J, Wei Q, She M, Marasco WA, Jiang H, Tu X, Zhu H, Ren L, Gao H,**
528   **Guo L, Huang L, Yang R, Cong Z, Wang Y, Liu Y, Sun Y, Duan S, Qu J, Chen L,**
529   **Tong W, Ruan L, Liu P, Zhang H, Zhang J, Liu D, Liu Q, Hong T, He W.** 2005. An
530   animal model of SARS produced by infection of Macaca mulatta with SARS coronavirus.
531   J Pathol **206:**251-259.
532   30.   **Rowe T, Gao G, Hogan RJ, Crystal RG, Voss TG, Grant RL, Bell P, Kobinger GP,**
533   **Wivel NA, Wilson JM.** 2004. Macaque model for severe acute respiratory syndrome. J
534   Virol **78:**11401-11404.
535   31.   **Shirato K, Kawase M, Matsuyama S.** 2013. Middle East respiratory syndrome
536   coronavirus infection mediated by the transmembrane serine protease TMPRSS2. J Virol
537   **87:**12552-12561.
538   32.   **Bertram S, Dijkman R, Habjan M, Heurich A, Gierer S, Glowacka I, Welsch K,**
539   **Winkler M, Schneider H, Hofmann-Winkler H, Thiel V, Pohlmann S.** 2013.
540   TMPRSS2 activates the human coronavirus 229E for cathepsin-independent host cell
541   entry and is expressed in viral target cells in the respiratory epithelium. J Virol **87:**6150-
542   6160.
543   33.   **Glowacka I, Bertram S, Muller MA, Allen P, Soilleux E, Pfefferle S, Steffen I,**
544   **Tsegaye TS, He Y, Gnirss K, Niemeyer D, Schneider H, Drosten C, Pohlmann S.**
545   2011. Evidence that TMPRSS2 activates the severe acute respiratory syndrome
546   coronavirus spike protein for membrane fusion and reduces viral control by the humoral
547   immune response. J Virol **85:**4122-4134.
548   34.   **Matsuyama S, Nagata N, Shirato K, Kawase M, Takeda M, Taguchi F.** 2010.
549   Efficient activation of the severe acute respiratory syndrome coronavirus spike protein by
550   the transmembrane protease TMPRSS2. J Virol **84:**12658-12664.
551   35.   **Letko M, Marzi A, Munster V.** 2020. Functional assessment of cell entry and receptor
552   usage for SARS-CoV-2 and other lineage B betacoronaviruses. Nat Microbiol
553   doi:10.1038/s41564-020-0688-y.
554   36.   **Schneider WM, Chevillotte MD, Rice CM.** 2014. Interferon-stimulated genes: a
555   complex web of host defenses. Annu Rev Immunol **32:**513-545.
556   37.   **Zhao X, Li J, Winkler CA, An P, Guo JT.** 2018. IFITM Genes, Variants, and Their
557   Roles in the Control and Pathogenesis of Viral Infections. Front Microbiol **9:**3228.

558 38. **Chen D, Hou Z, Jiang D, Zheng M, Li G, Zhang Y, Li R, Lin H, Chang J, Zeng H,**
559   **Guo JT, Zhao X.** 2019. GILT restricts the cellular entry mediated by the envelope
560   glycoproteins of SARS-CoV, Ebola virus and Lassa fever virus. Emerg Microbes Infect
561   **8:**1511-1523.
562 39. **Liu SY, Aliyari R, Chikere K, Li G, Marsden MD, Smith JK, Pernet O, Guo H,**
563   **Nusbaum R, Zack JA, Freiberg AN, Su L, Lee B, Cheng G.** 2013. Interferon-inducible
564   cholesterol-25-hydroxylase broadly inhibits viral entry by production of 25-
565   hydroxycholesterol. Immunity **38:**92-105.
566 40. **Shu Q, Lennemann NJ, Sarkar SN, Sadovsky Y, Coyne CB.** 2015. ADAP2 Is an
567   Interferon Stimulated Gene That Restricts RNA Virus Entry. PLoS Pathog **11:**e1005150.
568 41. **Yu J, Liu SL.** 2019. Emerging Role of LY6E in Virus-Host Interactions. Viruses **11**.
569 42. **Zhao X, Guo F, Liu F, Cuconati A, Chang J, Block TM, Guo JT.** 2014. Interferon
570   induction of IFITM proteins promotes infection by human coronavirus OC43. Proc Natl
571   Acad Sci U S A **111:**6756-6761.
572 43. **Zhao X, Sehgal M, Hou Z, Cheng J, Shu S, Wu S, Guo F, Le Marchand SJ, Lin H,**
573   **Chang J, Guo JT.** 2018. Identification of Residues Controlling Restriction versus
574   Enhancing Activities of IFITM Proteins on Entry of Human Coronaviruses. J Virol **92**.
575 44. **Sussman NL, Chong MG, Koussayer T, He DE, Shang TA, Whisennand HH, Kelly**
576   **JH.** 1992. Reversal of fulminant hepatic failure using an extracorporeal liver assist device.
577   Hepatology **16:**60-65.
578 45. **van Wenum M, Adam AA, Hakvoort TB, Hendriks EJ, Shevchenko V, van Gulik**
579   **TM, Chamuleau RA, Hoekstra R.** 2016. Selecting Cells for Bioartificial Liver Devices
580   and the Importance of a 3D Culture Environment: A Functional Comparison between the
581   HepaRG and C3A Cell Lines. Int J Biol Sci **12:**964-978.
582 46. **Yu J, Liang C, Liu SL.** 2019. CD4-Dependent Modulation of HIV-1 Entry by LY6E. J
583   Virol **93**.
584 47. **Yu J, Liang C, Liu SL.** 2017. Interferon-inducible LY6E Protein Promotes HIV-1
585   Infection. J Biol Chem **292:**4674-4685.
586 48. **Mar KB, Rinkenberger NR, Boys IN, Eitson JL, McDougal MB, Richardson RB,**
587   **Schoggins JW.** 2018. LY6E mediates an evolutionarily conserved enhancement of virus
588   infection by targeting a late entry step. Nat Commun **9:**3603.
589 49. **Waheed AA, Ablan SD, Soheilian F, Nagashima K, Ono A, Schaffner CP, Freed EO.**
590   2008. Inhibition of human immunodeficiency virus type 1 assembly and release by the
591   cholesterol-binding compound amphotericin B methyl ester: evidence for Vpu
592   dependence. J Virol **82:**9776-9781.
593 50. **Brown DA, London E.** 2000. Structure and function of sphingolipid- and cholesterol-
594   rich membrane rafts. J Biol Chem **275:**17221-17224.
595 51. **Chazal N, Gerlier D.** 2003. Virus entry, assembly, budding, and membrane rafts.
596   Microbiol Mol Biol Rev **67:**226-237, table of contents.
597 52. **Lin TY, Chin CR, Everitt AR, Clare S, Perreira JM, Savidis G, Aker AM, John SP,**
598   **Sarlah D, Carreira EM, Elledge SJ, Kellam P, Brass AL.** 2013. Amphotericin B
599   increases influenza A virus infection by preventing IFITM3-mediated restriction. Cell
600   Rep **5:**895-908.
601 53. **Godfrey DI, Masciantonio M, Tucek CL, Malin MA, Boyd RL, Hugo P.** 1992.
602   Thymic shared antigen-1. A novel thymocyte marker discriminating immature from
603   mature thymocyte subsets. J Immunol **148:**2006-2011.

604   54.   **Saitoh S, Kosugi A, Noda S, Yamamoto N, Ogata M, Minami Y, Miyake K,**
605   **Hamaoka T.** 1995. Modulation of TCR-mediated signaling pathway by thymic shared
606   antigen-1 (TSA-1)/stem cell antigen-2 (Sca-2). J Immunol **155:**5574-5581.
607   55.   **Bacquin A, Bireau C, Tanguy M, Romanet C, Vernochet C, Dupressoir A,**
608   **Heidmann T.** 2017. A Cell Fusion-Based Screening Method Identifies
609   Glycosylphosphatidylinositol-Anchored Protein Ly6e as the Receptor for Mouse
610   Endogenous Retroviral Envelope Syncytin-A. J Virol **91**.
611   56.   **Langford MB, Outhwaite JE, Hughes M, Natale DRC, Simmons DG.** 2018. Deletion
612   of the Syncytin A receptor Ly6e impairs syncytiotrophoblast fusion and placental
613   morphogenesis causing embryonic lethality in mice. Sci Rep **8:**3961.
614   57.   **Buchrieser J, Degrelle SA, Couderc T, Nevers Q, Disson O, Manet C, Donahue DA,**
615   **Porrot F, Hillion KH, Perthame E, Arroyo MV, Souquere S, Ruigrok K, Dupressoir**
616   **A, Heidmann T, Montagutelli X, Fournier T, Lecuit M, Schwartz O.** 2019. IFITM
617   proteins inhibit placental syncytiotrophoblast formation and promote fetal demise.
618   Science **365:**176-180.
619   58.   **Zani A, Zhang L, McMichael TM, Kenney AD, Chemudupati M, Kwiek JJ, Liu SL,**
620   **Yount JS.** 2019. Interferon-induced transmembrane proteins inhibit cell fusion mediated
621   by trophoblast syncytins. J Biol Chem **294:**19844-19851.
622   59.   **Rabbani MA, Ribaudo M, Guo JT, Barik S.** 2016. Identification of Interferon-
623   Stimulated Gene Proteins That Inhibit Human Parainfluenza Virus Type 3. J Virol
624   **90:**11145-11156.
625   60.   **Wilkins C, Woodward J, Lau DT, Barnes A, Joyce M, McFarlane N, McKeating JA,**
626   **Tyrrell DL, Gale M, Jr.** 2013. IFITM1 is a tight junction protein that inhibits hepatitis C
627   virus entry. Hepatology **57:**461-469.
628   61.   **Huang IC, Bailey CC, Weyer JL, Radoshitzky SR, Becker MM, Chiang JJ, Brass**
629   **AL, Ahmed AA, Chi X, Dong L, Longobardi LE, Boltz D, Kuhn JH, Elledge SJ,**
630   **Bavari S, Denison MR, Choe H, Farzan M.** 2011. Distinct patterns of IFITM-mediated
631   restriction of filoviruses, SARS coronavirus, and influenza A virus. PLoS Pathog
632   **7:**e1001258.
633   62.   **Feeley EM, Sims JS, John SP, Chin CR, Pertel T, Chen LM, Gaiha GD, Ryan BJ,**
634   **Donis RO, Elledge SJ, Brass AL.** 2011. IFITM3 inhibits influenza A virus infection by
635   preventing cytosolic entry. PLoS Pathog **7:**e1002337.
636   63.   **Yu J, Murthy V, Liu SL.** 2019. Relating GPI-Anchored Ly6 Proteins uPAR and CD59
637   to Viral Infection. Viruses **11**.
638   64.   **Jiang D, Guo H, Xu C, Chang J, Gu B, Wang L, Block TM, Guo JT.** 2008.
639   Identification of three interferon-inducible cellular enzymes that inhibit the replication of
640   hepatitis C virus. J Virol **82:**1665-1678.
641   65.   **Weidner JM, Jiang D, Pan XB, Chang J, Block TM, Guo JT.** 2010. Interferon-
642   induced cell membrane proteins, IFITM3 and tetherin, inhibit vesicular stomatitis virus
643   infection via distinct mechanisms. J Virol **84:**12646-12657.
644   66.   **Jiang D, Weidner JM, Qing M, Pan XB, Guo H, Xu C, Zhang X, Birk A, Chang J,**
645   **Shi PY, Block TM, Guo JT.** 2010. Identification of five interferon-induced cellular
646   proteins that inhibit west nile virus and dengue virus infections. J Virol **84:**8332-8341.
647   67.   **Chang J, Warren TK, Zhao X, Gill T, Guo F, Wang L, Comunale MA, Du Y, Alonzi**
648   **DS, Yu W, Ye H, Liu F, Guo JT, Mehta A, Cuconati A, Butters TD, Bavari S, Xu X,**

649   **Block TM.** 2013. Small molecule inhibitors of ER alpha-glucosidases are active against
650   multiple hemorrhagic fever viruses. Antiviral Res doi:10.1016/j.antiviral.2013.03.023.

651 68. **Lin HX, Feng Y, Tu X, Zhao X, Hsieh CH, Griffin L, Junop M, Zhang C.** 2011.
652   Characterization of the spike protein of human coronavirus NL63 in receptor binding and
653   pseudotype virus entry. Virus Res **160:**283-293.

654 69. **Zhao X, Guo F, Comunale MA, Mehta A, Sehgal M, Jain P, Cuconati A, Lin H,**
655   **Block TM, Chang J, Guo JT.** 2015. Inhibition of endoplasmic reticulum-resident
656   glucosidases impairs severe acute respiratory syndrome coronavirus and human
657   coronavirus NL63 spike protein-mediated entry by altering the glycan processing of
658   angiotensin I-converting enzyme 2. Antimicrob Agents Chemother **59:**206-216.

659 70. **He J, Choe S, Walker R, Di Marzio P, Morgan DO, Landau NR.** 1995. Human
660   immunodeficiency virus type 1 viral protein R (Vpr) arrests cells in the G2 phase of the
661   cell cycle by inhibiting p34cdc2 activity. J Virol **69:**6705-6711.

662 71. **Connor RI, Chen BK, Choe S, Landau NR.** 1995. Vpr is required for efficient
663   replication of human immunodeficiency virus type-1 in mononuclear phagocytes.
664   Virology **206:**935-944.

665 72. **Guo F, Zhao X, Gill T, Zhou Y, Campagna M, Wang L, Liu F, Zhang P, DiPaolo L,**
666   **Du Y, Xu X, Jiang D, Wei L, Cuconati A, Block TM, Guo JT, Chang J.** 2014. An
667   interferon-beta promoter reporter assay for high throughput identification of compounds
668   against multiple RNA viruses. Antiviral Res **107:**56-65.

669

670   **Figure and Figure legend**

671
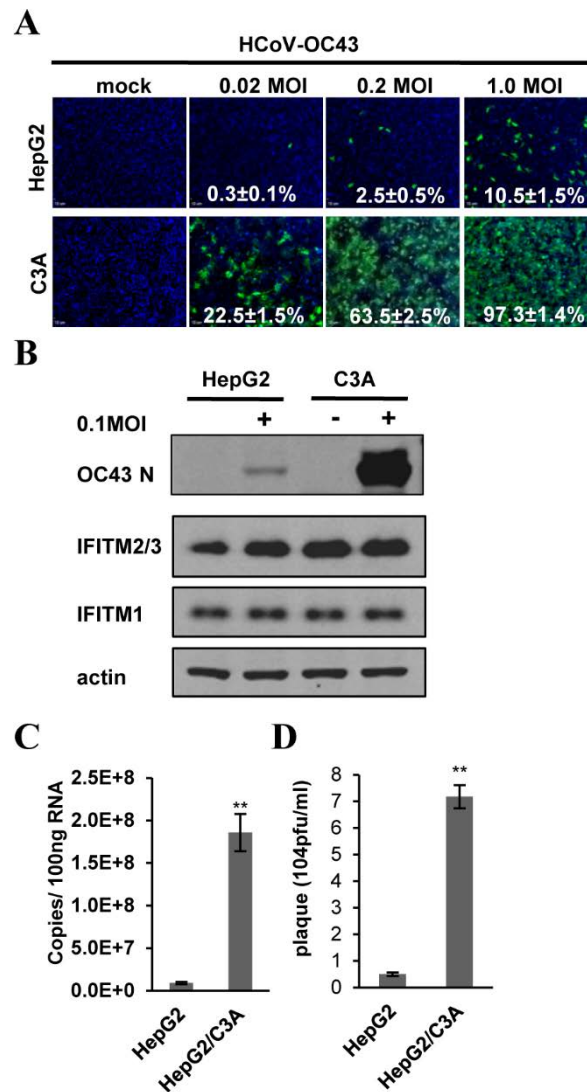
672

673   **Fig. 1. C3A cells are more susceptible to HCoV-OC43 infection than HepG2 cells.** HepG2
674   and C3A cells were mock-infected or infected with HCoV-OC43 at the indicated M.O.I. (**A**)
675   Cells were fixed at 24 h post infection (hpi) and infected cells were visualized by indirect
676   immunofluorescence (IF) staining of HCoV-OC43 N protein (green). Cell nuclei were visualized
677   by DAPI staining. (**B**) HCoV-OC43 NP, IFITMs and β-actin were determined by Western blot
678   assays. (**C**) Intracellular viral RNA was quantified by qRT-PCR assay and presented as copies
679   per 100 ng total RNA. Error bars indicate standard deviations (n = 4). (D) Viral yields were
680   determined with a plaque assay. Error bars indicate standard deviations (n = 4). ** indicates *p*
681   <0.001 (student *t* test).

27

682

683

684

685

686

687

688

689
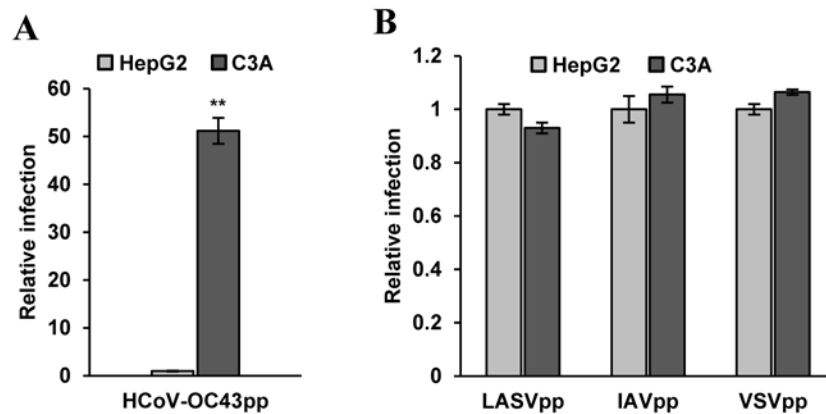
Fig. 2. C3A cells support more efficient entry of lentiviral particles pseudotyped with HCoV-OC43 envelope proteins than HepG2 cells. HepG2 and C3A cells were infected with HCoV-OC43pp (A), IAVpp, VSVpp or LASVpp (B). Luciferase activities were determined at 72 hpi. Relative infection represents the luciferase activity from C3A normalized to that of HepG2 cells. Error bars indicate standard deviations (n = 6). ** indicates $p < 0.001$ (student t test).

695

696

697

28

698

699
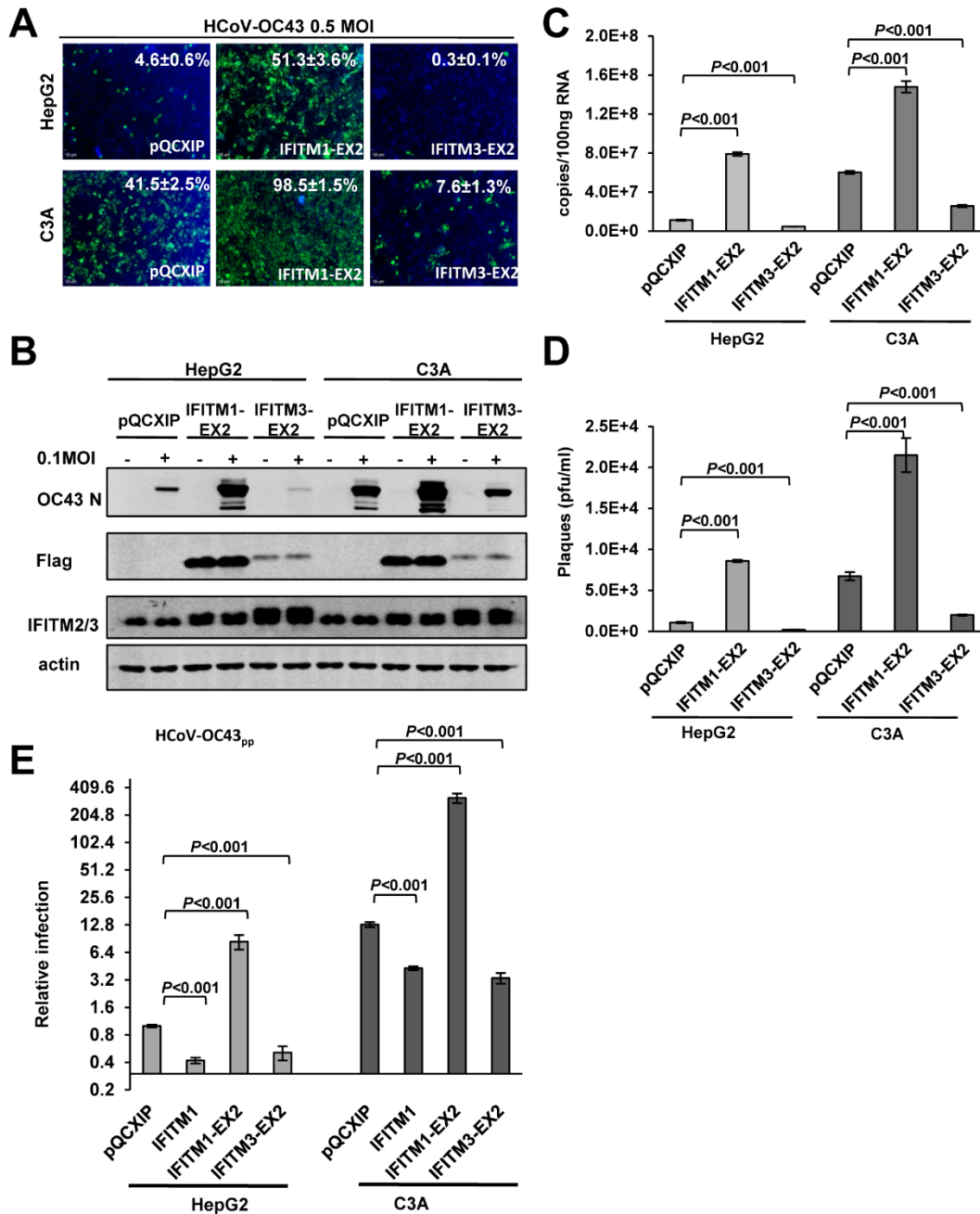
Fig. 3. IFITMs modulate HCoV-OC43 infection of HepG2 and C3A cells in a similar extent and *via* the same mechanism. HepG2 and C3A were stably transduced with a control retroviral vector (pQCXIP) or a retroviral vector expressing a N-terminally flag tagged IFITM1-EX2 or IFITM3-EX2. The resulting cell lines were infected with HCoV-OC43 at 0.1 MOI. (**A**) Cells were fixed at 24 hpi and virally infected cells were visualized by IF staining of HCoV-

29

705   OC43 N protein (green). Cell nuclei were visualized by DAPI staining. (**B**) HCoV-OC43 NP and
706   IFITM were determined by Western blot assays. β-actin served as a loading control. (**C**)
707   Intracellular viral RNA was quantified by a qRT-PCR assay and presented as copies per 100 ng
708   total RNA. Error bars indicate standard deviations (n = 4). (**D**) Viral yields were determined with
709   a plaque assay. Error bars indicate standard deviations (n = 4). (E) HepG2 and C3A stably
710   transduced with a control retroviral vector (pQCXIP) or a retroviral vector expressing IFITM1,
711   IFITM1-EX2 or IFITM3-EX2 were infected with HCoV-OC43pp. Luciferase activities were
712   determined at 72 hpi. Relative infection represents the luciferase activity normalized to that of
713   HepG2 cells transduced with empty vector (pQCXIP). Error bars indicate standard deviations (n
714   = 6).

715

716

717

718
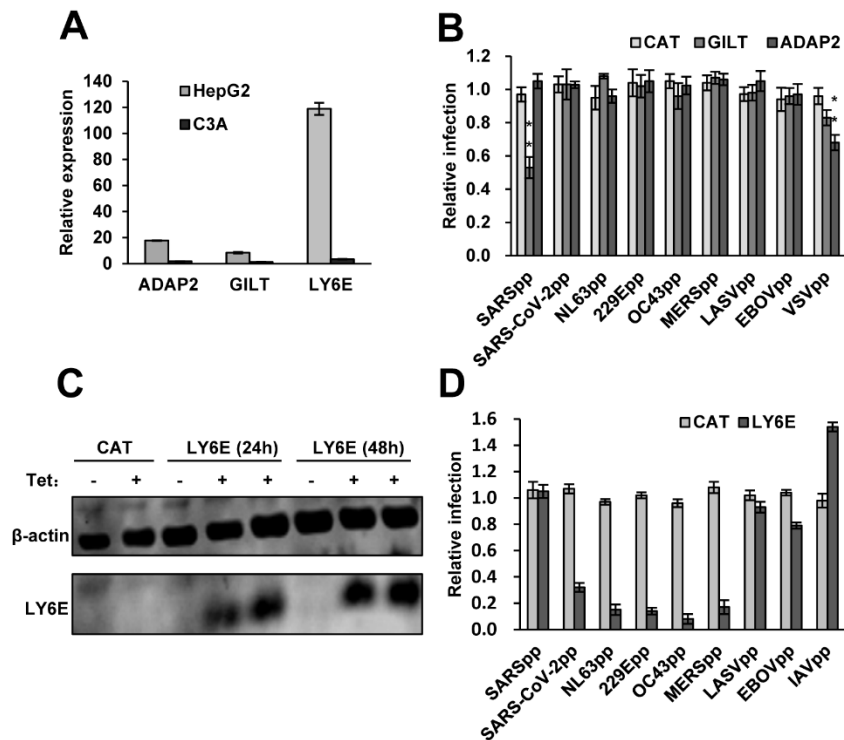
Fig. 4. LY6E efficiently suppresses human coronavirus spike protein-mediated entry. (A) Levels of Ly6E, GILT and ADAP2 mRNA expression in HepG2 and C3A cells were determined by qRT-PCR assays and normalized to the level of GAPDH. (B) Flp-In T-Rex 293-derived cell lines expressing control protein CAT, GILT or ADAP2 were cultured in the absence or presence of tet for 24 h. The cells were infected with HCoV-OC43pp and other indicated pseudoviral particles and intracellular luciferase activity were determined at 48 hpi. Relative infection is the ratio of luciferase activity in the same cells cultured in the presence of tet over that in the absence of tet. The error bars refer to standard deviations (n=4). (C) Flp-In T-Rex 293-derived cell line expressing a control protein CAT or LY6E were cultured in the absence or presence of tet. Cells were harvested at the indicated time after the addition of tet. Intracellular expression of LY6E was detected by a Western blot assay. β-actin served as a loading control. (D) Flp-In T-Rex 293-derived cell lines expressing LY6E were cultured in the absence or presence of tet for 24 h. The cells were then infected with lentiviral particles pseudotyped with the envelope protein of the indicated viruses. Luciferase activities were determined at 48 hpi. Relative infection is the ratio of luciferase activity in the same cells cultured in the presence of tet over that in the absence of tet. The error bars refer to standard deviations (n=4). **, $p < 0.001$ compared to the control cells expressing CAT.

736

31

737


738
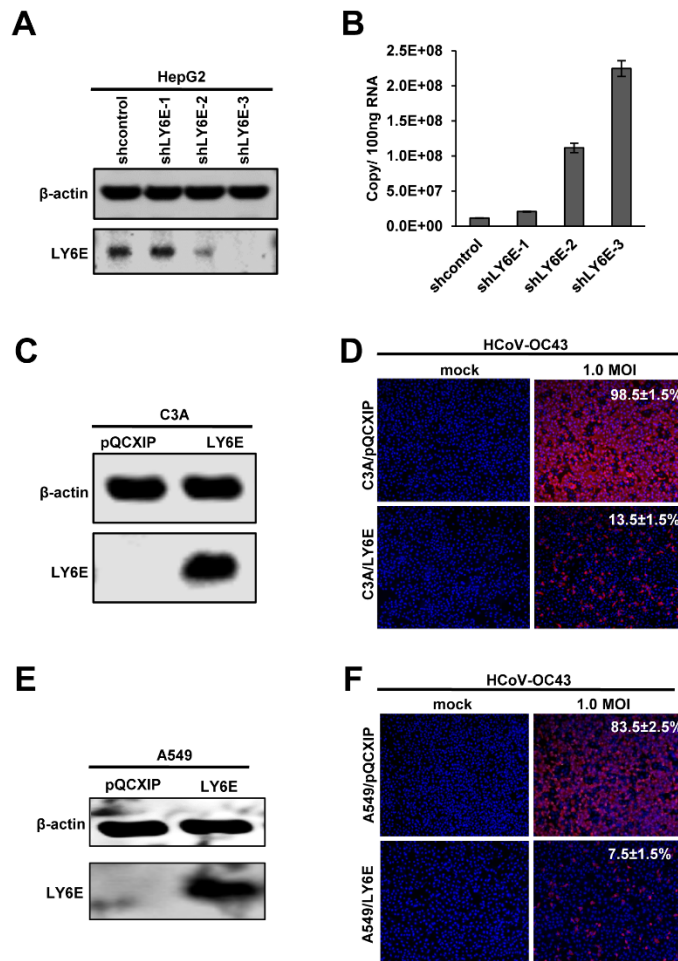
Fig. 5 LY6E inhibits HCoV-OC43 infection in human hepatoma (HepG2 and C3A) and lung cancer (A549) cells. (A) HepG2 cells were stably transduced with scramble shRNA or shRNA targeting LY6E mRNA. The level of intracellular LY6E expression was determined by Western blot using a rabbit polyclonal antibody against LY6E. β-actin served as a loading control. (B) HepG2 cells stably expressing the scramble shRNA or LY6E specific shRNA were infected with HCoV-OC43 at an MOI of 1.0. Cells were harvested at 24 hpi and intracellular viral RNA was quantified by qRT-PCR assay and presented as copies per 100 ng total RNA. Error bars indicate standard deviations (n = 4). (C to F) C3A or A549 cells were stably transduced with an empty retroviral vector (pQCXIP) or retroviral vector expressing LY6E and infected with HCoV-OC43 at the indicated MOI. The expression of LY6E in the cell lines was confirmed by a western blot assay. β-actin served as a loading control (C and E). The cells were fixed at 24 hpi. The infected cells were visualized by IF staining of HCoV-OC43 N protein (red). Cell nuclei were visualized by DAPI staining (D and F).

32

752

753
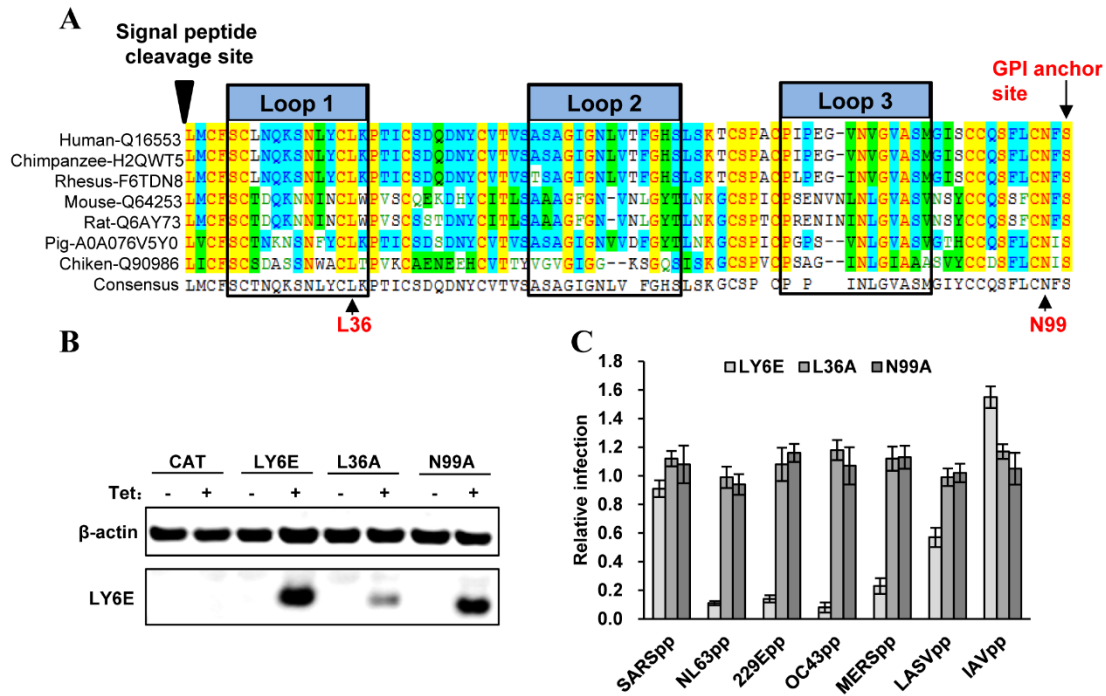
Fig. 6. Identification of critical structure motifs essential for LY6E to restrict human coronavirus entry. (A) The amino acid sequence alignment of LY6E from multiple vertebrate species is conducted and "three finger-fold" structure is highlighted with black box. The conserved L36 as well as GPI anchor and N99 glycosylation sites are indicated (B) Flp-In T-Rex 293-derived cell lines expressing a control protein CAT, wild-type or mutant LY6E were cultured in the absence or presence of tet for 24 h. Intracellular LY6E expression were detected by a Western blot assay. β-actin served as a loading control. (C) Flp-In T-Rex 293-derived cell lines expressing the wild-type or mutant LY6E were cultured in the absence or presence of tet for 24 h. The cells were then infected with the indicated pseudotyped lentivirus. Luciferase activities were measured at 48hpi. Relative infection is the ratio of luciferase activity in the same cells cultured in the presence of tet over that in the absence of tet. The error bars refer to standard deviations (n=4).

766

767

768

33

769

770
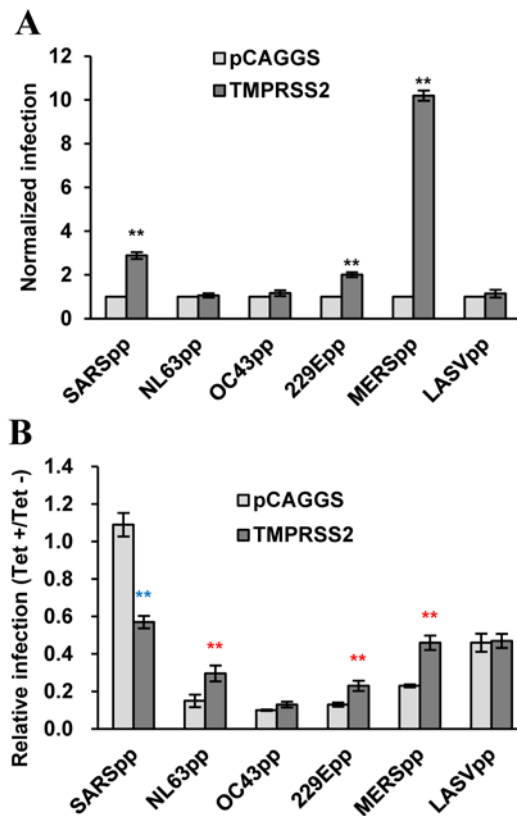
Fig. 7. LY6E inhibits TMPRSS2 enhanced entry of human coronaviruses. Flp-In T-Rex 293-derived cell line expressing LY6E were transfected with a control vector (pCAGGS) or a plasmid expressing human TMPRSS2 and cultured in the absence or presence of tet for 24 h. The cells were then infected with the indicated pseudotyped lentivirus. Luciferase activities were measured at 48hpi. (**A**) The effect of TMPRSS2 expression on pseudotyped virus infection is normalized to infection efficiency of the cells transfected with control vector plasmid (set as 1). Error bars indicate the standard deviation (n=4). (**B**) Relative infection refers to the ratio of the luciferase activity in the cells cultured in the presence of tet over that in the cells cultured in the absence of tet. Error bars indicate the standard deviation (n=4). **, p <0.001, comparing to cells transfected with pCAGGS vector.
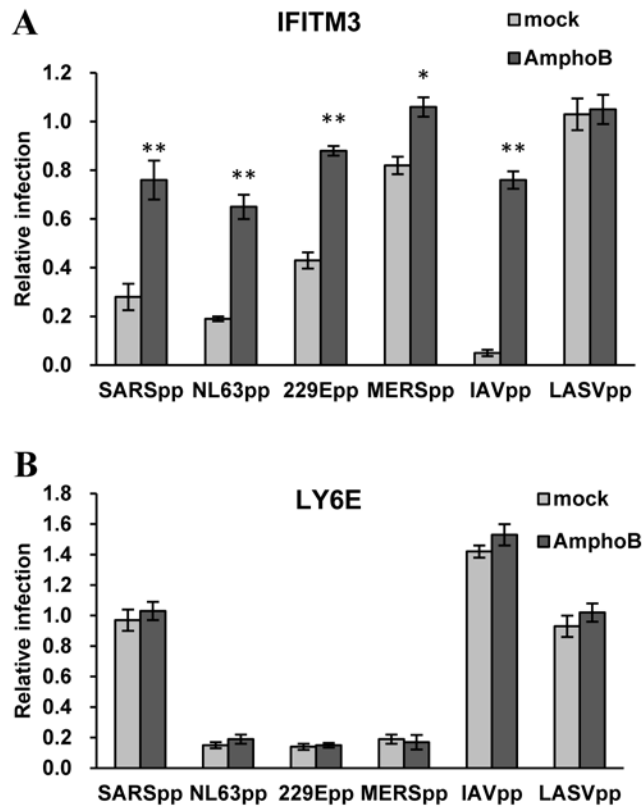
781

782

783

784

785

786

Fig. 8. Amphotericin B treatment compromises IFITM3 inhibition of human coronavirus entry, but have no impact on Ly6E inhibition of human coronavirus entry. Flp-In T-Rex 293-derived cell line expressing IFITM3 (**A**) or LY6E (**B**) were cultured in the absence or presence of tet for 24 h. The cells were then infected with the indicated pseudotyped lentivirus in the presence or absence of 1μM AmphoB. Luciferase activity was measured at 48 hr post-infection. Relative infection is the ratio of luciferase activity in the same cells cultured in the presence of tet over that in the absence of tet. The error bars refer to standard deviations (n=4). **, $p < 0.001$, compared to mock treatment.